## Title

Effect of Frustrated Rotations on the Pre-Exponential Factor for Unimolecular Reactions on Surfaces: A Case Study of Alkoxy Dehydrogenation



## Journal

The Journal of Physical Chemistry C, 124(2)

## ISSN

1932-7447

## Authors

Chen, Wei
Sun, Lixin
Kozinsky, Boris
et al.

## Publication Date

2020-01-16

## DOI

10.1021/acs.jpcc.9b10017

# The effect of frustrated rotations on the pre-exponential factor for unimolecular reactions on surfaces: a case study of alkoxy dehydrogenation

Wei Chen,[†,‡] Lixin Sun,[‡] Boris Kozinsky,[‡] Cynthia M. Friend,[¶,‡] Efthimios Kaxiras,[†,‡] Philippe Sautet,[§,‖] and Robert J. Madix[*,‡]

†*Department of Physics, Harvard University, Cambridge, MA 02138, USA*

‡*John A. Paulson School of Engineering and Applied Science, Harvard University, Cambridge, MA 02138, USA*

¶*Department of Chemistry and Chemical Biology, Harvard University, Cambridge, MA, 02138, USA*

§*Department of Chemical and Biomolecular Engineering, University of California, Los Angeles, California 90095, United States*

‖*Department of Chemistry and Biochemistry, University of California, Los Angeles, California 90095, United States*

E-mail: rmadix@seas.harvard.edu

**Abstract**

If theory is to be able to predict the rates of catalytic reactions over extended ranges of temperature and pressure, it must provide accurate rate constants for elementary reaction steps, including both the activation energy and pre-exponential factor. A standing difficulty with this objective is the treatment of floppy modes in the partition function for the adsorbed species. This issue leads to limited accuracy in the pre-exponential factor computed for realistic systems. Here we investigate the C–H bond breaking for a series of linear-chain alkoxides on Cu(110) using density functional theory, since the results can be compared to experimental data for the rate constants. The structural similarity of these species enables us to understand the systematic effect of molecular size on the frustrated motions and pre-exponential factor. First, we discuss the complexities of finding the global minimum structure of the adsorbed species and highlight the high dimensionality of configuration space to be sampled. Then, we analyze the motions of harmonic normal modes, including the motions of the underlying metal atoms, and compute the harmonic pre-exponential factors. To account for periodic frustrated rotations we use the hindered rotor model: this motion significantly decreases the pre-exponential factor in the C–H bond breaking, the effect increasing with molecular size. We also estimate the anharmonic effect using the Morse treatment of potentials. The activation energy and pre-exponential factor computed for $CH_3O$ are in excellent quantitative agreement with experiment. The trends computed for the homologous series of alcohols are also reflected by experiment.

# Introduction

A great amount of energy is consumed worldwide to produce industrially important chemicals, such as ammonia ($NH_3$), ethylene ($C_2H_4$), and formaldehyde ($CH_2O$). Reducing the energy cost of producing these chemicals by catalyst improvement is crucial for environmental sustainability.[1–3] From a mechanistic perspective, production of chemicals usually involves multiple elementary steps on the catalytic surfaces.[4] Each step is a state-to-state transition

that involves bond breaking and bond forming. For example, the anhydrous production of formaldehyde from methanol dehydrogenation requires O–H and C–H bond breaking with reformation of a H–H bond.[5,6] The competition between these reaction steps determines the production rates of the products. Accurate knowledge of the reaction rate constant of each elementary step allows the construction of kinetic models and assessment of the degree to which each step influences the rate and product selectivity,[7–9] which is important to the discovery and design of optimal catalysts for chemical production with low energy cost.[10]

The accurate prediction of the reaction rate constant ($k$), and separately the activation energy and pre-exponential factor, of an elementary step is non-trivial. Derived from transition state theory (TST), the Eyring equation[11] $k = \frac{k_\mathrm{B}T}{h}\frac{Q^\mathrm{TS}_\mathrm{vib}}{Q^\mathrm{RS}_\mathrm{vib}} \cdot \exp(-E_\mathrm{act}/k_\mathrm{B}T)$. $k$ depends exponentially on the difference in zero-point energy levels (electronic energies with zero-point vibrational energy corrections) between the reactant and transition states. Alternative calculations of $k$ require an exhaustive sampling of the configuration space by molecular dynamics (MD) or Monte Carlo (MC) simulations. Because of the high dimensionality of the configuration space, this sampling is computationally quite demanding for *ab initio* calculations, and thus only feasible for systems with reliable force fields. To accelerate the sampling, a history-dependent bias potential can be added to certain degrees of freedom (known as collective variables), as demonstrated in the methods such as metadynamics[12] and umbrella sampling.[13] However, choosing an appropriate set of collective variables, the core for a successful biased sampling, is system-specific and usually requires a substantial trial-and-error process. Furthermore, such calculations may or may not provide accurate values of the two kinetic parameters for comparison with experiment, which by definition are evaluated relative to the zero-point energy levels of reactants and transition state.

An alternative and more practical approach is often used to estimate these quantities from *ab initio* calculations. In the first step of this approach, transition state search methods are used to find the reaction path for a specific reaction and the coordinates of transition state, which give the activation electronic energy. In the second step, harmonic frequencies ($\nu$)

of the normal modes are calculated for the reactant and transition states, which give the zero-point vibrational energy (ZPE) and the vibrational partition functions ($Q_{\mathrm{vib}}$).[14] $Q_{\mathrm{vib}}$ is used to calculate the activation entropy ($\Delta S$) and thus the pre-exponential factor ($A$). $k$ can then be estimated from the Arrhenius equation: $k = A \cdot \exp(-E_{\mathrm{act}}/k_{\mathrm{B}}T)$, where $k_{\mathrm{B}}$ is the Boltzmann constant and $T$ is the temperature. A key drawback in this approach is that, the potentially significant frustrated rotational motion and anharmonicities in the low-frequency modes are neglected, whereas these modes may make large contributions to $Q_{\mathrm{vib}}$.[15] This deficiency may lead to errors in the predicted pre-exponential factor. To overcome the shortcoming, methods have been proposed to consider anharmonicity and frustrated motion. For example, Sauer *et al.* have proposed to independently sample the potential of each normal mode in the curvilinear internal coordinates, and use a high-order polynomial to fit the potential. The obtained anharmonic potentials are then used to calculate $Q_{\mathrm{vib}}$.[16–18] Campbell *et al.* have proposed to treat the lowest-frequency normal modes as hindered translations and rotations for adsorbed *molecular* species. Assuming the potentials that hinder such motions are sinusoidal, the partition functions of these modes can be estimated from the energy barriers of translation/rotation.[19,20]

Despite these developments in the estimation of pre-exponential factors, most kinetic studies of surface reactions still use empirical values of $10^{13}$ $\mathrm{s}^{-1}$,[21,22] leading to limited understanding of the factors that determine the pre-exponential factor in realistic systems. In this work we focus on the C–H bond breaking for a series of linear-chain alkoxides on Cu(110), including methoxy, ethoxy, 1-propoxy, and 1-butoxy. Their structural similarity allows the exploration of the effects of the molecular size on the frustrated motion and pre-exponential factor.

We estimate the pre-exponential factor from the harmonic frequencies of the reactant and transition states, treating the lowest frequency frustrated rotation by the hindered rotor model.[19,20] The atomic displacements in the low frequency normal modes are visualized to confirm the validity of this model. As the molecular size increases, there is a significant

increase in the partition function of the frustrated rotation of the adsorbed reactant and a corresponding lowering of the pre-exponential factor. The pre-exponential factor decreases by a factor of three progressing from methoxy to 1-butoxy. These results show the direction for future analysis.

# Methods

The major parameters used in our density functional theory (DFT) calculations, including simulation package, pseudopotentials, energy cutoff of plane-wave basis sets, van der Waals (vdW) corrections, slab structures, and $k$-point mesh, were the same as those in our earlier study.[6] In this study the structures of reactant and transition states in the C–H bond breaking process were converged to a very small force threshold (0.001 eV/Å). The Hessian matrix was calculated by the finite difference method. Four displacements, with a step size of 0.01 Å, were applied along each Cartesian coordinate of Cu atoms in the top layer and adsorbate atoms. The harmonic frequencies and mass-weighted Cartesian displacement of the normal modes were obtained from diagonalization of the *mass-weighted* Hessian matrix. The rotational barriers of the alkoxides were calculated by the climbing image nudged elastic band (CI-NEB) method[23] with seven intermediate images along each pathway and the Dimer method.[24] The atomic structures and *mass-unweighted* displacement of the normal modes were visualized by VESTA.[25]

# Results and Discussion

## Multiple basins in the energy landscape of adsorption

To estimate the pre-exponential factor, the first step is to identify the reactant-state structure at the *global minimum* energy. As the molecular size increases from methoxy to 1-butoxy, the dimensionality of the configuration space of adsorption increases quickly,

making the comprehensive sampling of the potential energy surface almost impossible with standard DFT calculations. Practically, several trial structures are often used to sample the configuration space, which lead to the discovery of several local basins in the energy landscape after structural relaxation. However, this searching approach does not ensure the identification of the global minimum.

Several stable/metastable structures were found for each larger alkoxide adsorbed on Cu(110). In previous work the *lowest energy structure* for each alkoxide was determined.[6] These structures were confirmed to be stable/metastable by harmonic frequency analysis. In the present study, as we explored the rotational motions of alkoxide on the surface (see the following section), structures with lower energies were found for 1-propoxy and 1-butoxy. The most stable adsorption configurations for the four alkoxides are shown in Fig. 1. The configurations of methoxy and ethoxy remain unchanged compared to those previously reported.[6] The newly discovered structures were more stable by 0.02 and 0.08 eV/molecule for 1-propoxy and 1-butoxy, respectively. Such energy stabilization is associated with the variation in the orientation of the molecule tail with respect to the $\beta$-C–O axis. The overall height of the alkoxy from the surface is also lowered in the new orientation. The distance between the backbone of the species and the Cu surface increases when the vdW interactions were excluded, confirming the significant vdW effects on the structures.[26–31]

The transition states for C–H bond breaking of 1-propoxy and 1-butoxy were reexamined with the updated adsorption structures. The NEB calculations suggested that the transition state structures remain unchanged compared to the previously reported ones (TS2 in Figs. 4 and 5 of Ref. 6). The activation barriers are given in Fig. 1 with updates in the values for 1-propoxy and 1-butoxy due to the change of the lowest energy state of the reactant. The activation energy for C–H bond cleavage increases nonmonotonically with molecular size for the alkoxy species with more than one carbon. The qualitative difference between methoxy and the other alkoxides is, however, quite significant. Excluding methoxy, an increase in the activation energy as the molecular size increases was observed.

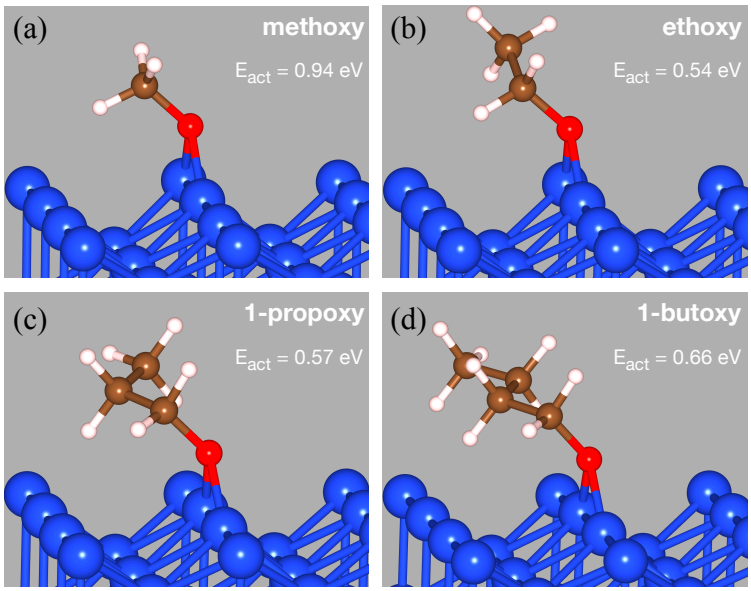


Figure 1: The most stable adsorption configurations of (a) methoxy, (b) ethoxy, (c) 1-propoxy, and (d) 1-butoxy on Cu(110), along with their respective C–H bond breaking barrier ($E_{\mathrm{act}}$).

It is important to emphasize more generally the difficulty in finding the global minimum in the high-dimensional configuration space of adsorption for large molecules. The searching strategy used previously for these alkoxides,[6] in which the molecule was considered as *a rigid body* and different adsorption sites and orientations of the molecule around its chemical bond with the surface were probed, may not be sufficient to find the structure at the global minimum energy because bending in the molecular skeleton and rotation around its internal bonds (torsion), which are common for adsorbed molecules, are extremely difficult to fully sample for large molecules. The abundance of local basins, potentially with multiple configurations with near-degenerate energies *highlight the difficulty to find the global minimum for an accurate estimation of kinetic parameters and other statistical quantities*, such as activation energy, entropy, and pre-exponential factor. Therefore, careful examination of structures is always needed for the quantitative description of the surface processes.

## Harmonic vibrational frequencies and partition functions

A wide range of harmonic frequencies for the normal modes of both reactant and transition states resulted from the frequency analysis. These are exemplified for methoxy and 1-butoxy in Fig. 2 (see Supporting Information for the data of other alkoxides). The numbers of atoms that are included in the construction of Hessian matrix are listed in Table 1. The inclusion of 12 Cu atoms in the topmost layer introduces 36 surface vibrational modes, in addition to the adsorbate vibrational modes, the number of which increases with molecule sizes. Because of the surface-adsorbate interaction, the surface and adsorbate vibrational modes can also couple to form normal modes with collective motions.

There are several major ranges in the frequency spectrum. (1) The frequencies above 2500 $cm^{-1}$ correspond to C–H stretch modes, the number of which increases from three for methoxy to nine for 1-butoxy at the reactant state. The transition state has one fewer frequency in this range than the reactant state due to the loss of the mode corresponding to the reaction coordinate. (2) There are no modes with frequencies within the range between 1500 and 2500 $cm^{-1}$. (3) The frequencies below 1500 $cm^{-1}$ and above about 250 $cm^{-1}$ mostly correspond to the bending and torsion motions internal to the adsorbate. As the molecular size increases, the number of modes within this intermediate range increases. (4) The frequencies between about 100 and 250 $cm^{-1}$ mostly correspond to the Cu surface modes, with relatively small displacement in the adsorbate atoms compared to other frequencies. The total number of frequencies within this range is close to 36. (5) The frequencies below about 100 $cm^{-1}$ mostly correspond to the coupled internal motions of adsorbates. There are three to four modes that have such low frequencies for each reactant- or transition-state structure. A Zip file is provided in Supporting Information that contains the normal mode displacement for each harmonic frequency (the displacement can be visualized by VESTA). The frequency structure for both the reactant and transition states appear nearly identical in Fig. 2. Thus, to the first approximation, the vibrational partition functions for the reactant and transition states would be expected to be quite similar.

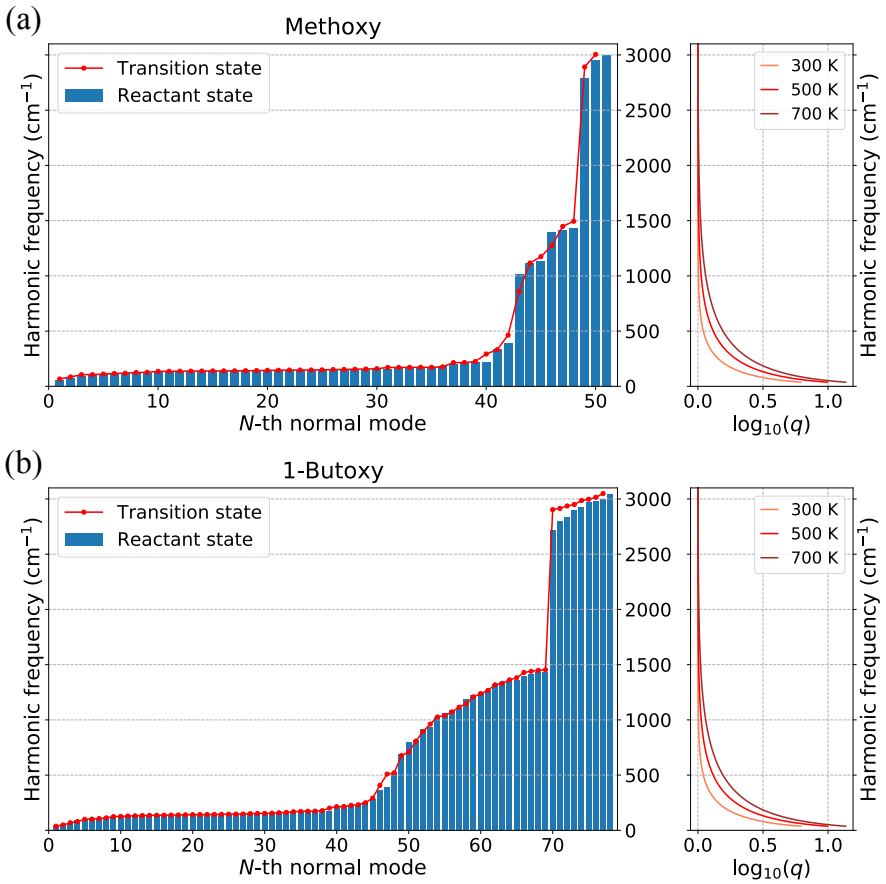


Figure 2: DFT-calculated harmonic frequencies (wavenumber, in cm$^{-1}$) of the normal modes of the reactant and transition states for C–H bond breaking of (a) methoxy and (b) 1-butoxy on Cu(110) (see Supporting Information for the results of ethoxy and 1-propoxy). The modes include the motion of Cu atoms in the topmost layer and are sorted in the ascending order of the frequencies. Subfigures on the right side, with the $y$-axis aligned with the left subfigures, show the dependence of harmonic partition function without ZPE term ($x$-axis, in $\log_{10}$ scale) on the harmonic frequencies ($y$-axis) at $T$ = 300, 500, and 700 K.

The harmonic pre-exponential factor $A$ for the reactions can then be estimated from the harmonic frequencies.[15]

$$A = \frac{k_{\mathrm{B}}T}{h} \cdot \frac{Q_{\mathrm{vib}}^{\mathrm{TS}}}{Q_{\mathrm{vib}}^{\mathrm{RS}}},$$

where $h$ is the Planck constant, and the vibrational partition function of the reactant state ($Q_{\mathrm{vib}}^{\mathrm{RS}}$) and transition state ($Q_{\mathrm{vib}}^{\mathrm{TS}}$) can be computed from $Q_{\mathrm{vib}} = \prod_j q_j^*$. For each mode, the quantum form of harmonic partition function with discrete energy levels,

$$q_j = \sum_{n=0}^{\infty} e^{-(n+\frac{1}{2})h\nu_j/k_{\mathrm{B}}T} = \frac{e^{-h\nu_j/2k_{\mathrm{B}}T}}{1 - e^{-h\nu_j/k_{\mathrm{B}}T}}$$

can be computed from its harmonic frequency $\nu_j$. The ZPE term in the numerator ($e^{-h\nu_j/2k_{\mathrm{B}}T}$) is included in the activation energy $E_{\mathrm{act}}$, and thus does not enter the pre-exponential factor. The validity of this approach is verified by the fact that the pronounced primary kinetic isotope effect observed for C–H bond breaking of $CH_3O$ on Cu(110) is entirely due to the difference in activation energies for $CH_3O$ and $CD_3O$. The primary factor to this difference is the ZPE of the CH(D) bonds in the methoxy.[32] The partition function without ZPE term

$$q_j^* = \frac{1}{1 - e^{-h\nu_j/k_{\mathrm{B}}T}}$$

is instead used to estimate $Q_{\mathrm{vib}}$, to avoid double counting of ZPE in the rate constant. Note that for low frequency modes $q_j^* \sim q_j + 0.5$. This can be seen by comparing $q_{\mathrm{har}}^*$ and $q_{\mathrm{har}}$ of the lowest frequency modes in Table 1.

The harmonic pre-exponential factor for the C–H bond breaking of each alkoxide increases with increasing molecular weight above methoxy and with increasing temperatures (Table 1). As temperature increases the pre-exponential factor becomes larger predominantly due to the $\frac{k_{\mathrm{B}}T}{h}$ term. As a reference, this term is equal to 6.25E+12, 1.04E+13, and 1.46E+13 at $T$ = 300, 500, and 700 K, respectively. The harmonic vibrational partition function $Q_{\mathrm{vib}}$ is smaller for the transition state than for the reactant state for each reaction, indicating *a*

*small loss of entropy in the transition state* as compared to the reactant state. This entropy decrease leads to a pre-exponential factor smaller than $k_{\mathrm{B}}T/h$ and for example nearly an order of magnitude smaller than $10^{13}$ s$^{-1}$ at 300 K, in sharp contrast to the commonly assumed value. Both ethoxy and 1-propoxy show smaller pre-exponential factors $A$ than methoxy, whereas the value for 1-butoxy is larger.

**Table 1: Quantities related to the harmonic frequencies for the reactant (RS) and transition (TS) states, including the number of atoms included in the construction of Hessian matrix (adsorbate and top-layer Cu), the number of real-frequency modes, the wavenumber ($\tilde{\nu}$) of the lowest frequency mode, the harmonic partition function of $\tilde{\nu}$ without ($q^*_{\mathrm{har}}$) and with ($q_{\mathrm{har}}$) ZPE term, and the partition function of $\tilde{\nu}$ estimated by the hindered rotor model ($q_{\mathrm{rot}}$) for RS. The harmonic ($A$) and corrected ($A'$, corrected by hindered rotor model) pre-exponential factors were calculated at 300, 500, and 700 K, respectively.**

| | | methoxy | | ethoxy | | 1-propoxy | | 1-butoxy | |
|---|---|---|---|---|---|---|---|---|---|
| | | RS | TS | RS | TS | RS | TS | RS | TS |
| # of atoms in Hessian | | 5(ads)+12(Cu) | | 8(ads)+12(Cu) | | 11(ads)+12(Cu) | | 14(ads)+12(Cu) | |
| # of real-freq modes | | 51 | 50 | 60 | 59 | 69 | 68 | 78 | 77 |
| lowest freq $\tilde{\nu}$ (cm$^{-1}$) | | 54 | 66 | 49 | 59 | 39 | 49 | 40 | 38 |
| $q^*_{\mathrm{har}}$ of $\tilde{\nu}$ (w/o ZPE) | 300 K | 4.40 | 3.67 | 4.80 | 4.03 | 5.81 | 4.74 | 5.72 | 6.04 |
| | 500 K | 6.98 | 5.75 | 7.65 | 6.36 | 9.34 | 7.55 | 9.19 | 9.72 |
| | 700 K | 9.57 | 7.84 | 10.50 | 8.70 | 12.87 | 10.36 | 12.66 | 13.41 |
| $q_{\mathrm{har}}$ of $\tilde{\nu}$ (with ZPE) | 300 K | 3.87 | 3.13 | 4.27 | 3.50 | 5.29 | 4.21 | 5.20 | 5.52 |
| | 500 K | 6.46 | 5.23 | 7.13 | 5.84 | 8.83 | 7.03 | 8.68 | 9.21 |
| | 700 K | 9.05 | 7.32 | 9.99 | 8.18 | 12.36 | 9.85 | 12.15 | 12.90 |
| $q_{\mathrm{rot}}$ of $\tilde{\nu}$ (with ZPE) | 300 K | 3.87 | – | 6.96 | – | 12.85 | – | 17.21 | – |
| | 500 K | 6.78 | – | 12.14 | – | 22.59 | – | 30.09 | – |
| | 700 K | 9.83 | – | 17.62 | – | 32.53 | – | 43.62 | – |
| harmonic pre-factor $A$ | 300 K | 2.70E+12 | | 1.31E+12 | | 1.61E+12 | | 5.92E+12 | |
| | 500 K | 3.95E+12 | | 1.82E+12 | | 2.25E+12 | | 9.15E+12 | |
| | 700 K | 5.23E+12 | | 2.37E+12 | | 2.92E+12 | | 1.23E+13 | |
| corrected pre-factor $A'$ | 300 K | 2.70E+12 | | 8.02E+11 | | 6.62E+11 | | 1.79E+12 | |
| | 500 K | 3.77E+12 | | 1.07E+12 | | 8.81E+11 | | 2.64E+12 | |
| | 700 K | 4.82E+12 | | 1.35E+12 | | 1.11E+12 | | 3.42E+12 | |

Deviations of the pre-exponential factor from $k_{\mathrm{B}}T/h$ are mainly determined by the low frequency modes in either the reactant or transition state. The vibrational partition function for high frequencies is unity, therefore the one extra C–H stretch mode in the reactant state makes little contribution to $Q^{\mathrm{TS}}_{\mathrm{vib}}/Q^{\mathrm{RS}}_{\mathrm{vib}}$. The largest contribution comes from *the variation of low frequency modes* in the reactant and transition states. For example, the lowest frequency mode of methoxy has a harmonic frequency of 54 cm$^{-1}$ in the reactant state and 66 cm$^{-1}$

in the transition state (Table 1). This small difference of 12 $cm^{-1}$ is hardly visible in Fig. 2, but it contributes $q^{*TS}_{har}/q^{*RS}_{har} \sim 0.8$ to $Q^{TS}_{vib}/Q^{RS}_{vib}$ (differences between $q^{*TS}_{har}$ and $q^{*RS}_{har}$ increase slowly as temperature becomes higher). For each alkoxide, there are a few modes that have frequency $< 100$ $cm^{-1}$, and their difference in the reactant and transition states largely determines the pre-exponential factor. At higher temperatures, more modes are involved in this determination. Also 1-butoxy exhibits a mode with frequency $\sim 500$ $cm^{-1}$ that differs by $\sim 100$ $cm^{-1}$ between the reactant and transition states (Fig. 2b, see Supporting Information for normal mode displacements). For all these dehydrogenation reactions the contribution made by breaking the C–H bond is more than 80% of the ZPE difference. This value varies from almost 100% to $\sim 80\%$ for 1-butoxy. In the latter case the remaining 20% comes from other high-frequency modes (Fig. 2). The low-frequency modes ($< 500$ $cm^{-1}$) contribute less than 5% in all cases, even for 1-butoxy.

Despite the high sensitivity of partition function to the low frequency modes, the potential errors in DFT-predicted harmonic frequencies from Hessian matrix are far beyond a few $cm^{-1}$. More importantly, *the anharmonic effects and the periodicity of frustrated motions* in the low frequency modes due to the local symmetry of the binding site are not captured by the Hessian matrix method. Therefore, achieving an accurate estimation of the pre-exponential factor, especially for large adsorbates where the low frequency modes are abundant, is extremely difficult.

## The effects of frustrated translations and rotations

Both the reactant and transition states have motions identifiable as frustrated rotations and translations which contribute to the pre-exponential factor. The frustrated translations correspond to vibrations ($x, y, z$ motions) of the center of mass with respect to the binding site. The frustrated rotational motions, on the other hand, correspond to rotation of the adsorbed specie around an axis, which experiences a periodic potential. To address these degrees of freedom a model for hindered motion was employed.[19,20] For the desorption of weakly bound

molecules from surfaces Campbell *et al.* proposed that *the three lowest frequencies* computed for the adsorbed molecule from DFT calculations can be attributed to *two hindered translations and one hindered rotation*, whose partition functions can be estimated by assuming sinusoidal-shape potentials for the hindered motions.[33] For the alkoxy species under consideration here, the frustrated translations are the $x, y, z$ motions of the alkoxy resulting from the O–Cu binding and have frequencies well above 200 $cm^{-1}$. These frustrated translations are localized, and thus can be reasonably well described by the harmonic approximation.

The frustrated rotational motion of alkoxide on the surface is a low frequency mode, however. For this motion the atomic displacements in the lowest frequency mode of each higher molecular weight alkoxide (see the displacements in Fig. 3 and Supporting Information) look quite similar to the rotation of molecule around the out-of-plane axis through the short bridge site where the molecule is adsorbed (see the kinetic pathway in Fig. 4). The lowest frequency mode of methoxy more likely corresponds to rotation around an axis through the two Cu atoms bonded to oxygen, i.e., a frustrated rotation.

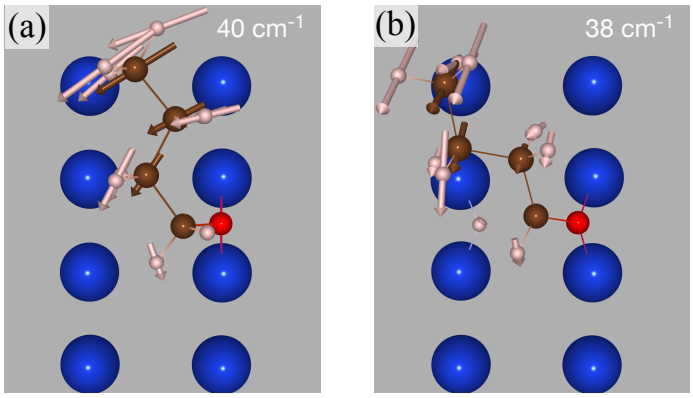


Figure 3: Displacements of atoms in the lowest frequency normal modes of the (a) reactant and (b) transition states for C–H bond breaking of 1-butoxy on Cu(110) (see Supporting Information for the results of other molecules). The harmonic frequencies are listed. Each arrow indicates the direction and relative amplitude of displacement of the atom that it penetrates through. Note that each displacement indicates angular motion around the vertical axis perpendicular to the surface through the O atom. The displacements of Cu atoms are too small to be visible.

Using this approach the partition functions of the lowest frequency rotational modes

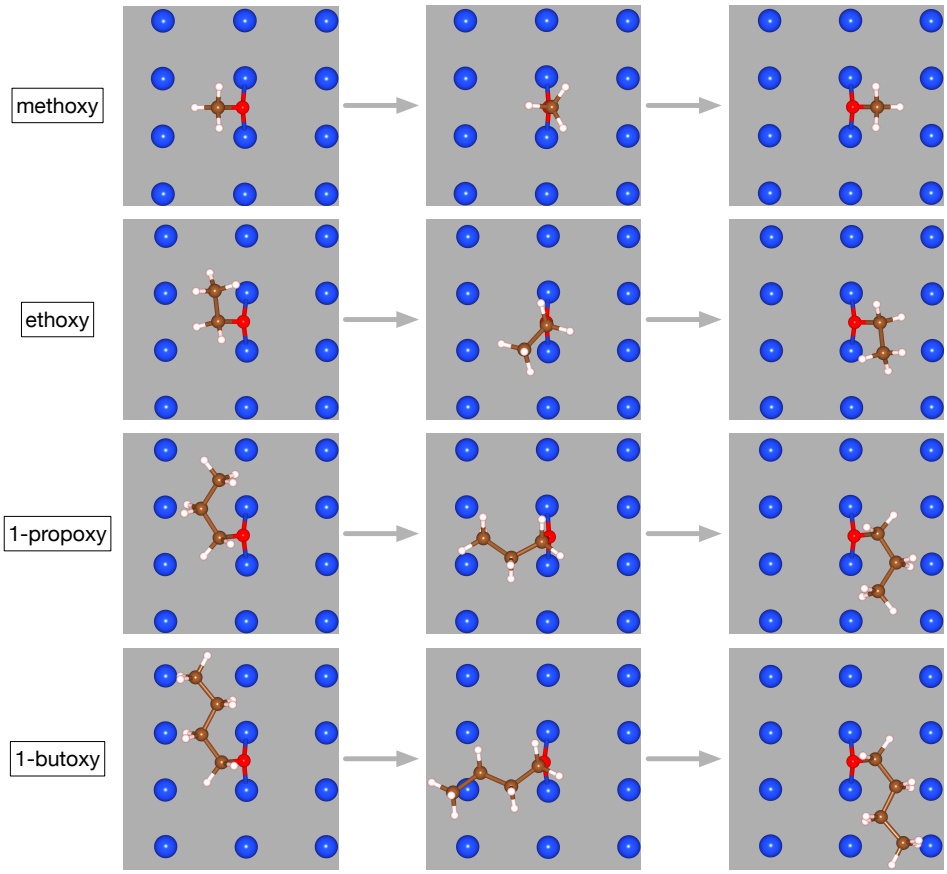


Figure 4: Top views of the minima and TS structures for the rotation of each alkoxide around the normal axis through the O atom on Cu(110). The transition states of the rotation are placed in the middle.

were estimated. This periodic rotation of adsorbate around the normal axis of the surface is *forbidden in the transition state* because the dissociating H atom connects the surface Cu atoms and the $\beta$-C atom. Therefore, this frustrated rotational mode was considered as a hindered rotor only for the reactant alkoxy state. We calculated the rotational barrier of each alkoxide around the surface normal axis (Fig. 4) using the NEB and Dimer methods. The internal relaxation of molecule was allowed without applying a rigid body approximation. The barriers, $W_r$, are within the small range of 0.12–0.16 eV and do not show any significant size dependence (Fig. 5a). The fact that $W_r$ does not change significantly with molecular size suggests a relatively small contribution to $W_r$ from the interaction between the tail of the molecule and the surface. This interaction may not change much in magnitude for the alkoxy at different rotational angles. The reduced moment of inertia $I$ was calculated from the mass of each adsorbate atom and the distance from each adsorbate atom to the surface normal axis extending through the adsorption site. $I$ values calculated from the adsorption structures of alkoxides were used and approximated to be unchanged during rotation. Note that the angle ($\theta$) between the normal and the O–C bond can vary upon rotation, so $I(\theta)$ is not constant and *our treatment of rigid rotation is an approximation*, especially for the case of methoxy. $I$ increases quickly as the molecular size is enlarged (Fig. 5a).

The hindered rotor partition function $q_{\mathrm{rot}}$ was calculated from these values of $W_r$ and $I$.[19] The values of $q_{\mathrm{rot}}$ and the harmonic partition function $q_{\mathrm{har}}$ (calculated from harmonic frequency $\nu_j$) for each alkoxide at 300, 500, and 700 K are listed in Table 1. The formulation of $q_{\mathrm{rot}}$ includes the ZPE contribution, so we compare $q_{\mathrm{rot}}$ with $q_{\mathrm{har}} = \frac{e^{-h\nu_j/2k_{\mathrm{B}}T}}{1-e^{-h\nu_j/k_{\mathrm{B}}T}}$ instead of with $q^*_{\mathrm{har}} = \frac{1}{1-e^{-h\nu_j/k_{\mathrm{B}}T}}$. For methoxy the harmonic approximation seems to well describe the lowest frequency mode ($q_{\mathrm{rot}} \sim q_{\mathrm{har}}$, see Fig. 5b). As the molecular size increases, the difference between $q_{\mathrm{rot}}$ and $q_{\mathrm{har}}$ rises sharply. Since the rotational barrier is small, the hindered rotor is an excellent model for low frequency rotational modes. Therefore, the harmonic approximation greatly underestimates the rotational partition function for larger species that can rotate relatively freely, which would apply to many adsorbed reaction intermediates. At

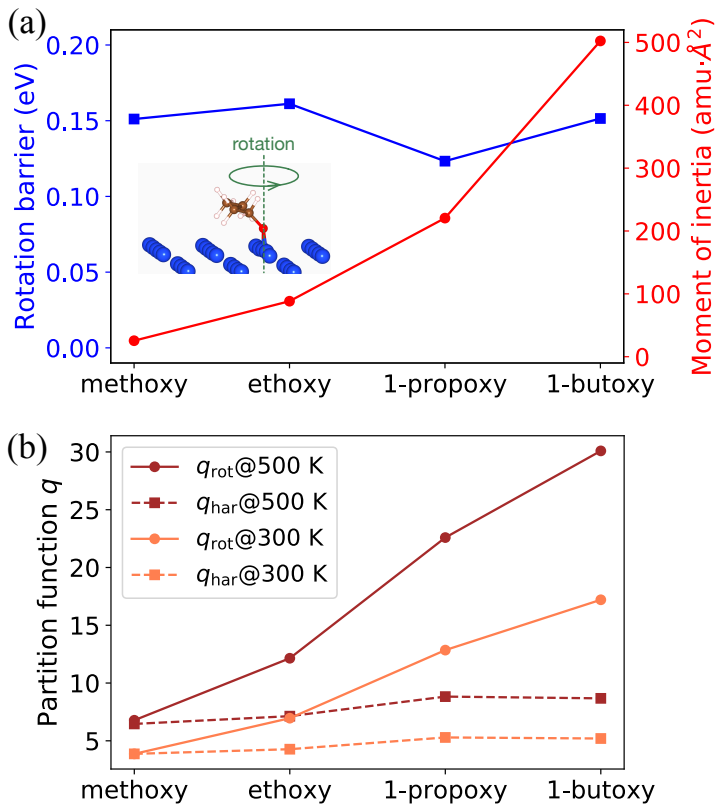


Figure 5: Frustrated rotation of alkoxide around the normal axis on Cu(110) treated by the hindered rotor model. (a) Rotation barrier $W_r$ and reduced moment of inertia $I$ for each alkoxide. The inset is a schematic of the periodic frustrated rotation of alkoxide. (b) The partition function of the lowest frequency rotational mode calculated by the hindered rotor model ($q_{\mathrm{rot}}$, solid lines) compared with the harmonic partition function ($q_{\mathrm{har}}$, dashed lines) at 300 and 500 K.

$T$ = 300 K, the correction factor $q_{\mathrm{rot}}/q_{\mathrm{har}}$ due to the effect of frustrated rotation is equal to 1.0, 1.6, 2.4, and 3.3 for methoxy, ethoxy, 1-propoxy, and 1-butoxy, respectively, showing *a clear size dependence*. The correction factor becomes slightly larger as temperature rises. For example, the factor increases from 3.3 at 300 K to 3.5 at 500 K, and to 3.6 at 700 K for 1-butoxy.

The correction in the partition function of the lowest frequency mode in the reactant state affects the estimated pre-exponential factor. Since the harmonic pre-exponential factor $A \propto 1/q^{\mathrm{RS}}$, the corrected pre-exponential factor reads

$$A' = A \cdot \frac{q_{\mathrm{har}}}{q_{\mathrm{rot}}}.$$

Here we used the correction factor $q_{\mathrm{rot}}/q_{\mathrm{har}}$ to correct $q^*_{\mathrm{har}}$ in $A$ because the formulation of $q_{\mathrm{rot}}$ includes the ZPE contribution. This treatment only causes negligible error because $q^*_{\mathrm{har}} \sim q_{\mathrm{har}}$ for low frequency modes. The corrected pre-exponential factors $A'$ are listed in Table 1. The values are substantially different from the harmonic pre-factors for ethoxy, 1-propoxy, and 1-butoxy. The corrected pre-factor of 1-butoxy is now smaller than that of methoxy. For example, at 300 K, the harmonic pre-factor for 1-butoxy is 5.92E+12, which is more than twice of that for methoxy (2.70E+12). The above correction reduces the pre-factor to 1.79E+12 for 1-butoxy, which is smaller than that for methoxy (2.70E+12, remain unchanged from the harmonic pre-factor).

So far we have focused on the frustrated rotation of the reactant around the surface normal. This motion is lost in the transition state because the adsorbate is "locked" by the nascent bond of H bridging between Cu and $\beta$-C. The hindered rotor model allowed us to better estimate the partition function of this motion. Note that although only this motion was treated by the hindered rotor model,[19,20] there are two other frustrated rotations, one around the $x$ and the other around the $y$ axis (both $x$ and $y$ axes are perpendicular to surface normal). These two rotations do not correspond to full (360°) rotations with periodic

angular potentials due to the existence of surface. Therefore, the hindered rotor model with a sinusoidal potential is not applicable to them.

To address the effect of these modes on the partition function we estimated the vibrational anharmonicity. The method developed by Sauer et al. was explored.[16] Under the independent mode approximation,[34] each mode was sampled using the *rectilinear* normal mode displacement.[16] Not surprisingly, the potential energy changes in low-frequency bending or torsional modes were overestimated, leading to underestimation of the partition function. This problem needs to be overcome by utilizing the *curvilinear displacements defined by internal coordinates*.[17,18] However, defining a set of internal coordinates, which requires careful tuning of parameters such as van der Waals radii, is very difficult for adsorbate-surface systems.

Instead we sampled the one-dimensional angular potentials of the two frustrated rotations for the four alkoxides (see Supporting Information). The curves were fitted by both harmonic and Morse potentials. For methoxy and ethoxy the two rotations can be reasonably well described by the harmonic potentials, with their fundamental frequencies not much different from those of the Morse potentials. For 1-propoxy and 1-butoxy the anharmonic feature of the potentials becomes more pronounced. Their curves can only be fitted well by the Morse potentials. This trend of increased anharmonic correction in larger molecules is similar to that established above for the periodic frustrated rotation around the surface normal. However, the anharmonic correction factor to the partition function due to the frustrated rotation around the $x$- or $y$-axis, which is up to 1.4 at 300 K, is much small than that due to the periodic rotation around the $z$-axis, which can be over 3 at 300 K. Therefore, the latter is the main focus of the present work. It is important to note that the angular potentials were evaluated by keeping the molecular species rigid at each angle, so some inaccuracy may exist in the calculation.

Though the literature contains very few accurately measured pre-exponential factors for elementary steps in surface reactions, rigorous studies of the rate constant for C–H bond

cleavage in methoxy on Cu(110) have been performed previously.[32] These measurements are sufficiently accurate to quantify the kinetic isotope effects for $CH_3O$, $CH_2DO$, $CHD_2O$, and $CD_3O$. The activation energy for C–H bond cleavage in methoxy on Cu(110) is 0.91 eV and the pre-exponential factor is 1.0E+12 $s^{-1}$. The computed values listed in Table 2 are in good agreement with the experimental values.

In addition, relative values of the rate constants for C–H bond cleavage in methoxy, ethoxy, propoxy, and butoxy have been determined by temperature programmed reaction spectroscopy.[29] Only for methoxy have the pre-exponential factor and activation energy been separately determined. The experimental values of the rate constant near 300 K are such that $k_{CH_3O} < k_{CH_3(CH_2)_3O} < k_{CH_3(CH_2)_2O} \sim k_{CH_3CH_2O}$, in agreement with the computed values (Table 2). The rate constant for methoxy is substantially lower than the others due to a qualitatively different geometric configuration of the transition state,[6] and the rate constant for butoxy is lower than those for ethoxy and propoxy due to slightly increased activation energy in higher molecular weight alkoxide among the three molecules.

**Table 2: DFT-calculated kinetic parameters for C–H bond cleavage, including the activation energies ($E_{act}$, in eV), the harmonic and corrected pre-exponential factors ($A$ and $A'$, in $s^{-1}$) and rate constants ($k$ and $k'$, in $s^{-1}$) at $T$ = 300 K.**

| | $E_{act}$ (w/o ZPE) | $E_{act}$ (with ZPE) | harmonic (300 K) | | corrected (300 K) | |
|---|---|---|---|---|---|---|
| | | | pre-factor $A$ | rate constant $k$ | pre-factor $A'$ | rate constant $k'$ |
| methoxy | 0.94 | 0.76 | 2.70E+12 | 4.61E−01 | 2.70E+12 | 4.61E−01 |
| ethoxy | 0.54 | 0.38 | 1.31E+12 | 5.41E+05 | 8.02E+11 | 3.31E+05 |
| 1-propoxy | 0.57 | 0.42 | 1.61E+12 | 1.42E+05 | 6.62E+11 | 5.82E+04 |
| 1-butoxy | 0.66 | 0.52 | 5.92E+12 | 1.09E+04 | 1.79E+12 | 3.29E+03 |

Besides the three frustrated rotations of the alkoxy species that contribute to lowering the magnitude of the pre-exponential factor, there are other low frequency modes with non-localized displacements of adsorbate atoms that may cause even further lowering if they do not have equivalent partners in the transition state. Identifying the motion for each mode from the displacement vectors on each atom and ensuring this motion is decoupled from other motions is quite difficult. In such systems with many floppy modes coupled, the lack of practical approaches to quantitatively and systematically treat frustrated motions and

anharmonicity requires method development beyond the scope of this paper. Qualitatively, we expect that, due to the “locking" effect (constrained degree of freedom along the reaction coordinate), several low frequency modes may lose substantial entropy in the transition state. The loss of entropy may not be properly captured by the harmonic approximation, leading to overestimation of the pre-exponential factor. The overestimation is expected to be more severe in larger adsorbates where the floppy modes are more abundant. The conclusion from this analysis is that the actual pre-exponential factor may be a factor of up to ten smaller than that which we have calculated.

Before closing, we emphasize that the present study considers low coverages of adsorbates on the (110) terrace of Cu. In reaction processes that involve high coverages of adsorbates, the inter-adsorbate coupling can have a significant effect on the surface motions of adsorbates and their entropy. Second, surface defects and steps may serve as the active sites, where the motions and entropy of adsorbate can be different from those on the terrace. The enhanced adsorption at these active sites usually leads to lowering of the freedom of adsorbate. The general reduction in the activation energy suggests that the transition state may lose more freedom than the reactant state does, leading to a smaller pre-exponential factor at the defect and step sites. Overall, the pre-exponential factor of surface reaction, which is related to the entropy change between the reactant and transition states, can be significantly affected by these two factors (adsorbate coverage and surface morphology). Currently we are exploring the effect of single-atom dopant (as the active site) on the motions of adsorbates and the pre-exponential factor of reaction process.

# Conclusions

In summary, the C–H bond breaking for a series of linear-chain alkoxides on Cu(110) has been studied to understand the effect of molecular size on the frustrated rotations and, hence, the pre-exponential factor. The pre-exponential factor was calculated using the harmonic

frequencies from the Hessian matrix. The accurate description of low-frequency modes is significant to the prediction of the pre-exponential factor. For higher accuracy hindered rotation was included to evaluate the lowest frequency rotational mode. The choice of this mode was confirmed by examination of the displacement vectors of numerous low frequency normal modes. Values of the pre-exponential factor lie close to $10^{12}$ $s^{-1}$ for all the reactions, varying by approximately a factor of two between the species. As the molecular size increases, the effect of periodic frustrated rotation becomes more significant, and its correction to the pre-exponential factor is more substantial. The present work provides insights into the key aspects that influence the pre-exponential factor in realistic systems. These insights can be helpful for the development of novel methods to accurately predict the reaction pre-exponential factor.

## Acknowledgements

This work was supported by the Integrated Mesoscale Architectures for Sustainable Catalysis, an Energy Frontier Research Center funded by the U.S. Department of Energy, Office of Science, Basic Energy Sciences under Award # DE-SC0012573. The calculations were performed at the the Oak Ridge Leadership Computing Facility (OLCF) and the National Energy Research Scientific Computing Center (NERSC) of the U.S. Department of Energy, and the Extreme Science and Engineering Discovery Environment (XSEDE).

## References

(1) Christensen, C. H.; Rass-Hansen, J.; Marsden, C. C.; Taarning, E.; Egeblad, K. The renewable chemicals industry. *ChemSusChem* **2008**, *1*, 283–289.

(2) Chu, S.; Cui, Y.; Liu, N. The path towards sustainable energy. *Nat. Mater.* **2017**, *16*, 16.

(3) Friend, C. M.; Xu, B. Heterogeneous catalysis: a central science for a sustainable future. *Acc. Chem. Res.* **2017**, *50*, 517–521.

(4) Campbell, C. T. Chemistry: Towards tomorrow's catalysts. *Nature* **2004**, *432*, 282.

(5) Li, H.-J.; Lausche, A. C.; Peterson, A. A.; Hansen, H. A.; Studt, F.; Bligaard, T. Using microkinetic analysis to search for novel anhydrous formaldehyde production catalysts. *Surf. Sci.* **2015**, *641*, 105–111.

(6) Chen, W.; Cubuk, E. D.; Montemore, M. M.; Reece, C.; Madix, R. J.; Friend, C. M.; Kaxiras, E. A Comparative Ab Initio Study of Anhydrous Dehydrogenation of Linear-Chain Alcohols on Cu (110). *J. Phys. Chem. C* **2018**, *122*, 7806–7815.

(7) Sabbe, M. K.; Reyniers, M.-F.; Reuter, K. First-principles kinetic modeling in heterogeneous catalysis: an industrial perspective on best-practice, gaps and needs. *Catal. Sci. Technol.* **2012**, *2*, 2010–2024.

(8) Reece, C.; Redekop, E. A.; Karakalos, S.; Friend, C. M.; Madix, R. J. Crossing the great divide between single-crystal reactivity and actual catalyst selectivity with pressure transients. *Nat. Catal.* **2018**, *1*, 852.

(9) Reece, C.; Luneau, M.; Madix, R. J. Dissecting the Performance of Nanoporous Gold Catalysts for Oxygen-Assisted Coupling of Methanol with Fundamental Mechanistic and Kinetic Information. *ACS Catal.* **2019**, *9*, 4477–4487.

(10) Nørskov, J. K.; Bligaard, T.; Rossmeisl, J.; Christensen, C. H. Towards the computational design of solid catalysts. *Nat. Chem.* **2009**, *1*, 37.

(11) Eyring, H. The activated complex in chemical reactions. *J. Chem. Phys.* **1935**, *3*, 107–115.

(12) Barducci, A.; Bonomi, M.; Parrinello, M. Metadynamics. *Wiley Interdiscip. Rev. Comput. Mol. Sci.* **2011**, *1*, 826–843.

(13) Torrie, G. M.; Valleau, J. P. Nonphysical sampling distributions in Monte Carlo free-energy estimation: Umbrella sampling. *J. Comput. Phys.* **1977**, *23*, 187–199.

(14) Henkelman, G.; Jónsson, H. Long time scale kinetic Monte Carlo simulations without lattice approximation and predefined event table. *J. Chem. Phys.* **2001**, *115*, 9657–9666.

(15) Campbell, C. T.; Árnadóttir, L.; Sellers, J. R. Kinetic prefactors of reactions on solid surfaces. *Z. Phys. Chem.* **2013**, *227*, 1435–1454.

(16) Piccini, G.; Sauer, J. Quantum chemical free energies: Structure optimization and vibrational frequencies in normal modes. *J. Chem. Theory Comput.* **2013**, *9*, 5038–5045.

(17) Piccini, G.; Sauer, J. Effect of anharmonicity on adsorption thermodynamics. *J. Chem. Theory Comput.* **2014**, *10*, 2479–2487.

(18) Piccini, G.; Alessio, M.; Sauer, J. Ab initio calculation of rate constants for molecule–surface reactions with chemical accuracy. *Angew. Chem. Int. Ed.* **2016**, *55*, 5235–5237.

(19) Sprowl, L. H.; Campbell, C. T.; Arnadottir, L. Hindered translator and hindered rotor models for adsorbates: Partition functions and entropies. *J. Phys. Chem. C* **2016**, *120*, 9719–9731.

(20) Campbell, C. T.; Sprowl, L. H.; Arnadottir, L. Equilibrium constants and rate constants for adsorbates: two-dimensional (2D) ideal gas, 2D ideal lattice gas, and ideal hindered translator models. *J. Phys. Chem. C* **2016**, *120*, 10283–10297.

(21) Reuter, K. First-principles kinetic Monte Carlo simulations for heterogeneous catalysis: Concepts, status, and frontiers. *Modeling Heterogeneous Catalytic Reactions: From the Molecular Process to the Technical System* **2011**, *3*, 71–111.

(22) Zuo, Z.-J.; Gao, X.-Y.; Han, P.-D.; Liu, S.-Z.; Huang, W. Density functional theory (DFT) and kinetic monte carlo (KMC) study of the reaction mechanism of hydrogen production from methanol on ZnCu (111). *J. Phys. Chem. C* **2016**, *120*, 27500–27508.

(23) Henkelman, G.; Uberuaga, B. P.; Jónsson, H. A climbing image nudged elastic band method for finding saddle points and minimum energy paths. *J. Chem. Phys.* **2000**, *113*, 9901–9904.

(24) Henkelman, G.; Jónsson, H. A dimer method for finding saddle points on high dimensional potential surfaces using only first derivatives. *J. Chem. Phys.* **1999**, *111*, 7010–7022.

(25) Momma, K.; Izumi, F. VESTA 3 for three-dimensional visualization of crystal, volumetric and morphology data. *J. Appl. Crystallogr.* **2011**, *44*, 1272–1276.

(26) Hiebel, F.; Shong, B.; Chen, W.; Madix, R. J.; Kaxiras, E.; Friend, C. M. Self-assembly of acetate adsorbates drives atomic rearrangement on the Au (110) surface. *Nat. Commun.* **2016**, *7*, 13139.

(27) Zhou, Y.; Chen, W.; Cui, P.; Zeng, J.; Lin, Z.; Kaxiras, E.; Zhang, Z. Enhancing the hydrogen activation reactivity of non-precious metal substrates via confined catalysis underneath graphene. *Nano Lett.* **2016**, *16*, 6058.

(28) Karakalos, S.; Xu, Y.; Kabeer, F. C.; Chen, W.; Rodríguez-Reyes, J. C. F.; Tkatchenko, A.; Kaxiras, E.; Madix, R. J.; Friend, C. M. Non-Covalent Bonding Controls Selectivity in Heterogeneous Catalysis: Coupling Reactions on Gold. *J. Am. Chem. Soc.* **2016**, *138*, 15243.

(29) Xu, Y.; Chen, W.; Kaxiras, E.; Friend, C. M.; Madix, R. J. General Effect of van der Waals Interactions on the Stability of Alkoxy Intermediates on Metal Surfaces. *J. Phys. Chem. B* **2017**, *122*, 555–560.

(30) Cheenicode Kabeer, F.; Chen, W.; Madix, R. J.; Friend, C. M.; Tkatchenko, A. First-Principles Study of Alkoxides Adsorbed on Au (111) and Au (110) Surfaces: Assessing the Roles of Non-Covalent Interactions and Molecular Structures in Catalysis. *J. Phys. Chem. C* **2017**,

(31) O'Connor, C. R.; Hiebel, F.; Chen, W.; Kaxiras, E.; Madix, R. J.; Friend, C. M. Identifying key descriptors in surface binding: interplay of surface anchoring and intermolecular interactions for carboxylates on Au(110). *Chem. Sci.* **2018**, *9*, 3759–3766.

(32) Madix, R.; Telford, S. Primary and secondary kinetic isotope effects for methoxy dehydrogenation and Cu (110): absence of tunnelling corrections. *Surf. Sci.* **1995**, *328*, L576.

(33) Hill, T. L. *An introduction to statistical thermodynamics*; Courier Corporation, 1986.

(34) Beste, A. One-dimensional anharmonic oscillator: Quantum versus classical vibrational partition functions. *Chem. Phys. Lett.* **2010**, *493*, 200–205.

# Graphical TOC Entry